Lorentzian symmetry predicts universality beyond scaling laws

Stephen J. Watson

School of Mathematics and Statistics, University of Glasgow, University Place, Glasgow G12 8SQ, SCOTLAND [(a)]

PACS 64.60.De – Statistical mechanics of model systems
PACS 05.70.Ln – Nonequilibrium and irreversible thermodynamics
PACS 05.65.+b – Self-organized systems

Abstract – We present a covariant theory for the ageing characteristics of *phase-ordering* systems that possess dynamical symmetries beyond mere scalings. A chiral spin dynamics which conserves the *spin-up* (+) and *spin-down* (−) fractions, μ_+ and μ_-, serves as the emblematic paradigm of our theory. Beyond a parabolic spatio-temporal scaling, we discover a *hidden* Lorentzian dynamical symmetry therein, and thereby prove that the characteristic length L of *spin domains* grows in time t according to $L = \frac{\beta}{\sqrt{1-\sigma^2}} t^{\frac{1}{2}}$, where $\sigma := \mu_+ - \mu_-$ (the invariant *spin-excess*) and β is a universal constant. Furthermore, the normalised length distributions of the spin-up and the spin-down domains each provably adopt a coincident universal (σ-independent) time-invariant form, and this *supra-universal* probability distribution is empirically verified to assume a form reminiscent of the *Wigner surmise*.

Introduction. – The statistical physics that govern either thermodynamic or *driven* phase-ordering dynamics [1, 2] continue to intrigue [3–14], while unifying principles have remained largely elusive. *Coarsening/Ageing* of the ensemble of *phase domains* is a key feature of such far-from-equilibrium dynamics, wherein irreversible annihilation or joining of domains yields a growing *characteristic domain length* L. Temporal power-laws $L \propto t^n$ ($n > 0$) that emerge at late-times t, alongside a concomitant *scale-invariance* of associated topological and morphological distributions, have so frequently been empirically observed that their presence has acquired the status of a principle; the *Dynamic-Scaling Hypothesis* [1, 15].

The Dynamic Scaling Hypothesis ($\mathcal{DSH}$) has not yet reached the status of the *scaling hypothesis* for *critical phenomena*, where the emergence of such scaling covariance has been theoretical explained via Wilson's seminal *renormalization group*. In addition, the violation of *fluctuation-dissipation relations*, which is generally associated with *driven* systems, furnishes a particularly far-reaching challenge to theoretical developments. Furthermore, the dynamical symmetries of a given coarsening (ageing) dynamical system - its *Coarsening Group* - may include more than mere global spatio-temporal scalings [16]: for example, the *Schrödinger group* encoding local scale-transformations has been hypothesised and studied in the context of physical ageing [17]. That said, the means to rationally identify how general coarsening groups are reflected in the statistical distributions of phase-ordering, has, till now, lacked a rigorous theoretical framework.

In this letter, we reveal how the symmetry group G of a *Coarsening (ageing) Dynamical System* ($\mathcal{CDS}$) necessarily yields G-equivariance (covariance) of the $\mathcal{CDS}$'s universal statistical parameters and probability distributions. We exhibit this *G-Equivariant Universality* for a chiral particle/anti-particle $\mathcal{CDS}$, which also encodes the conservative ordering dynamics of a driven 2-state spin system - *spin-up* (+) and *spin-down* (−) - evolving with invariant *spin-fractions* μ_+ and μ_-. The symmetry group G of this spin-domain dynamics is found to possess not only a $\mathbb{Z}_2$ inversion, $\mathbb{J}$, and parabolic spatio-temporal scalings, $\mathbb{P}_\lambda$, but also an additional family of *hidden Lorentzian boosts* $\mathbb{T}_\zeta$, where $\zeta \in (-1, 1)$. The *spin-excess* $\sigma := \mu_+ - \mu_- \in (-1, 1)$ is then shown to be a G-equivariant statistical invariant, which, in particular, is *boosted* by $\mathbb{T}_\zeta$, namely

$$\sigma \xrightarrow{\mathbb{T}_\zeta} \zeta \oplus \sigma \qquad \text{where} \quad \zeta \oplus \sigma := \frac{\zeta + \sigma}{1 + \zeta\sigma}. \tag{1}$$

We thereby prove that the characteristic length of spin domains L is governed at *late times* t by

$$L = \frac{\beta}{\sqrt{1-\sigma^2}} t^{\frac{1}{2}}, \tag{2}$$

[(a)] E-mail: Stephen.Watson@glasgow.ac.uk

where $\beta \approx 1.25$ is a universal constant. We also theoretically discover that the normalised distribution of domain lengths will, after a transient, be given by the time-independent probability density

$$\widehat{P}(l) = \frac{1}{2}\frac{1}{1+\sigma}\mathcal{W}\left(\frac{l}{1+\sigma}\right) + \frac{1}{2}\frac{1}{1-\sigma}\mathcal{W}\left(\frac{l}{1-\sigma}\right), \quad (3)$$

where the *supra-universal* normalised probability density $\mathcal{W}(l)$ is empirically determined to be a certain *hyperbolic deformation* of the *Wigner Surmise*.

Chiral Kink Dynamics. – We introduce here a chiral particle/anti-particle dynamics in one space dimension $\mathbb{R}$, for which *coarsening* (*ageing*) naturally occurs through irreversible annihilation events that arise when a particle/anti-particle pair meet. Our model point particle (*p-kink*) and its mirror-image counterpart, the anti-particle (*n-kink*), each carry a (*topological*) charge $q \in \{\pm 1\}$, with the p-kink being positively charged, $q = +1$, while the n-kink is negatively so, $q = -1$. It is natural to identify a *kink* k residing at $x \in \mathbb{R}$ with the signed *Dirac delta function (measure)* $q\delta_x$. Our model dynamics governs alternating arrays of such p- and n- kinks, wherein the instantaneous velocity $\mathcal{V} = \frac{dx}{dt}$ of any given kink $k = q\delta_x$ is determined by

$$q\mathcal{V} = \frac{1}{L_l} - \frac{1}{L_r}, \quad (4)$$

where L_l and L_r represent the distances to the kink's left- and right- neighbouring anti-kinks: see Fig. 1. Since the parity transformation $\mathcal{P}$ reflects a kink's location, $x \overset{\mathcal{P}}{\longrightarrow} -x$, while flipping the kink to its enantiomeric counterpart, $\overset{\mathcal{P}}{\rightleftarrows}$, it follows that $\mathcal{P}$ inverts both the kink's charge and velocity, namely $q \overset{\mathcal{P}}{\longrightarrow} -q$ and $\mathcal{V} \overset{\mathcal{P}}{\longrightarrow} -\mathcal{V}$, while also switching its left- and right- neighbour distances, i.e., $L_r \overset{\mathcal{P}}{\longleftrightarrow} L_l$. The kink dynamics (4) thereby transform under parity $\mathcal{P}$ into the (enantiomeric) mirror counterpart $q\mathcal{V} = \frac{1}{L_r} - \frac{1}{L_l}$.

The kink dynamics (4) stand in natural correspondence with a certain *conservative spin dynamics*,

$$\partial_t s + \partial_x J = 0, \quad (5)$$

in which a two-state *spin field* s in one space dimension evolves under a *spin flux* J that is induced by a constant applied field $E \neq 0$. Here, the *spin state* s occupying a given point $x \in \mathbb{R}$ at a particular time $t \geq 0$ is either *spin-up*, $s(x,t) = \frac{1}{2}$, or *spin-down*, $s(x,t) = -\frac{1}{2}$. Also, the spin flux J is presumed to be spatially uniform within any given *spin-up or spin-down domain* (see Fig. 2), taking on a value that is inversely proportional to the respective spin domain's length l, namely

$$J = -\frac{E}{l}. \quad (6)$$

The constant applied field E, which is either positively $(+)$ or negatively $(-)$ oriented, is naturally normalised through the simple rescaling of time $t \mapsto Et$, and so we may, without loss of generality, restrict $E = +1$ or $E = -1$. Note that this spin dynamics is neither invariant under field reversal $* : E \mapsto -E$, nor under the parity transformation $\mathcal{P}$, which flips the spin, $\pm\frac{1}{2} \mapsto \mp\frac{1}{2}$, reverses the field, $E \mapsto -E$, and inverts space, $x \mapsto -x$.

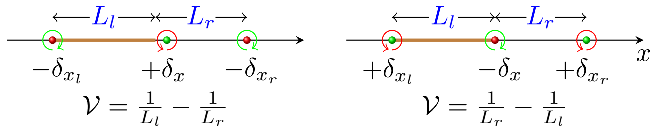

Fig. 1: Illustration of the chiral kink dynamics (4) in the case of either a p-kink at x, namely $+\delta_x$, or an n-kink at x, $-\delta_x$. Here, $\mathcal{V}$ denotes the kink velocity, $\mathcal{V} = \frac{\mathrm{d}x}{\mathrm{d}t}$, while $L_l := x - x_l$ and $L_r := x_r - x$ are the distances to left- and right-neighbouring anti-kinks respectively.

A *domain wall* (*shock front*) at $x \in \mathbb{R}$, which sits between adjacent spin-up and spin-down domains of s, necessarily moves with a velocity $\frac{\mathrm{d}x}{\mathrm{d}t}$ that satisfies the *Rankine-Hugoniot* relation

$$[\![s]\!]_x \frac{\mathrm{d}x}{dt} = [\![J]\!]_x, \quad (7)$$

where $[\![s]\!]_x := s(x^+) - s(x^-)$ and $[\![J]\!]_x := J(x^+) - J(x^-)$ encode the jump in the spin, and the spin-current, across the domain wall at x, respectively. Note that $[\![s]\!]_x \in \{\pm 1\}$ and $[\![J]\!]_x = E\left(\frac{1}{L_l} - \frac{1}{L_r}\right)$, with L_l and L_r being the distances from x to the left- and right- neighbouring domain walls. Now, imbuing each domain wall with a *wall charge* $q \in \{\pm 1\}$ according to

$$q := E\,[\![s]\!]_x \in \{\pm 1\}, \quad (8)$$

while noting (7), one then finds that

$$q\frac{\mathrm{d}x}{dt} = E\,[\![s]\!]_x \frac{\mathrm{d}x}{dt} = E^2\left(\frac{1}{L_l} - \frac{1}{L_r}\right) = \frac{1}{L_l} - \frac{1}{L_r}. \quad (9)$$

This naturally inspires one to view *domain walls* of s as *charged quasi-particles*, since such domain-walls necessarily follow the chiral kink dynamics (4), and thereby effectively act as p- and n- kinks.

The proportion of space occupied by the spin-up domains of s, denoted $\mu_+ \in (0,1)$, and also that of spin-down domains, $\mu_- \in (0,1)$, are invariants of the conservative spin dynamics (5). The kink dynamics (4) then inherits these invariants through the spin field associated with alternating kink arrays, as per Fig. 2. We will later see that the invariant *spin-excess*

$$\sigma := \mu_+ - \mu_- \in (-1,1), \quad (10)$$

which measures the imbalance between the *spin-up* and *spin-down fractions*, μ_+ and μ_-, completely parametrises the *universality classes* of coarsening kink ensembles

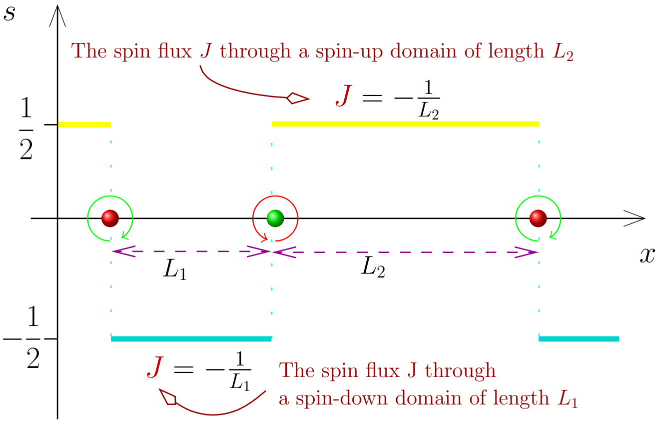

Fig. 2: Schematic of a two-state *spin-field*, $s \in \{\pm\frac{1}{2}\}$, in one dimensional space, $\mathbb{R}$, that is driven by an applied field $E = +1$ which induces a spin current J given by (6). The p- and n- kinks (and) are co-located according to their charge $q \in \{\pm 1\}$ at those *domain walls* of s with co-incident *wall charge*, as given by (8). The kink dynamics (4) then effectively governs the evolution of the spin-field s under the conservative dynamics (5).

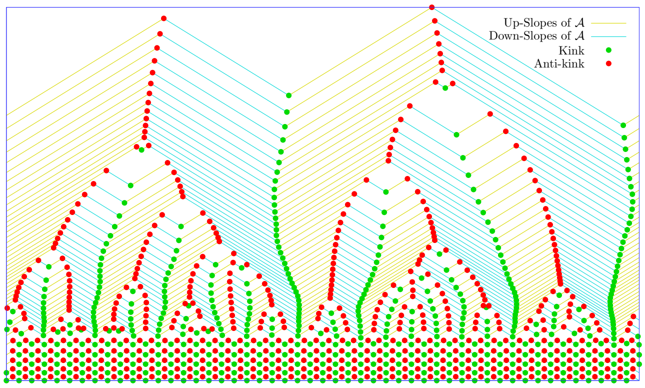

Fig. 3: A numerically computed solution $\mathcal{A}[t]$ of the Faceted-Oriented-Interface Dynamics ($\mathcal{FOID}$) (11) exhibited through spatial snapshots of $\mathcal{A}[t]$ at a representative sequence of times. The initial *saw-tooth* profile $\mathcal{A}[0]$ is generated by randomly perturbing a periodic profile.

The chiral coarsening kink dynamics (4) may also be naturally encoded within a one-dimensional faceted oriented interface $\mathcal{A}[t]$ that is dynamically evolving in time t as illustrated in Fig. 3. Here, $\mathcal{A}[t]$ is *dinormal*, with its two possible time-independent facet normals, say n_+ and n_-, being mutually perpendicular ($n_+ \perp n_-$), while the (instantaneous) normal velocity ν of each facet is determined solely by the reciprocal of the facet's current length l [13], namely

$$\nu = \frac{1}{l}. \tag{11}$$

A representative solution of this Faceted-Oriented-Interface Dynamics ($\mathcal{FOID}$) is exhibited in Fig. 3. By identifying the positive- and negative- curvature vertices (corners) of $\mathcal{A}[t]$ with p-kinks and n-kinks respectively, while viewing the facet length between vertices as the distance between kinks, it follows that the vertex evolution of $\mathcal{A}[t]$ naturally maps to the kink dynamics (4). Incidentally, the chirality of the kink dynamics (4) is clearly evidenced through the ternary coarsening motif appearing in Fig. 3, wherein two negative-curvature vertices (*n-kinks*) simultaneously coalesce with a positive-curvature vertex (*p-kink*) resulting in a new negative-curvature vertex (n-kink): a chiral motif, since the enantiomeric counterpart motif $+ 2$ $\to$ does not appear.

Dynamical Symmetries. We now turn to identifying the symmetry group G of the chiral kink dynamics (4), since G will play a key role in our later analysis of the universal parameters and probability distributions that emerge from coarsening ensembles of kinks. To begin, note that the composition of the parity transformation $\mathcal{P}$ with the *charge switch* $\overset{\star}{\leftrightharpoons}$ ($q \overset{\star}{\to} -q$), namely the *inversion* $\mathbb{J} := \mathcal{P}^\star$, acts on a kink $k = q\delta_x$ according to

$$\mathbb{J} \cdot k = \mathbb{J} \cdot q\delta_x = q\delta_{-x}. \tag{12}$$

Upon then noting $\mathcal{V} \overset{\mathbb{J}}{\to} -\mathcal{V}$, $q \overset{\mathbb{J}}{\to} q$ and $L_l \overset{\mathbb{J}}{\leftrightarrow} L_r$, one readily sees that $\mathbb{J}$ yields a Z_2 symmetry of (4). The spin dynamics (5) are likewise invariant under the inversion $\mathbb{J}$, which reflects space, $x \mapsto -x$, flips the spin, $\pm\frac{1}{2} \mapsto \mp\frac{1}{2}$, and preserves the field, $E \mapsto E$. Since $\mathbb{J}$ inverts the spin-field s, $s \overset{\mathbb{J}}{\to} -s$, it thereby also exchanges the associated spin fractions, μ_+ and μ_-, that is $\mu_\pm \overset{\mathbb{J}}{\to} \mu_\mp$. The spin-excess σ (10) is therefore inverted by $\mathbb{J}$, namely

$$\sigma \overset{\mathbb{J}}{\to} -\sigma. \tag{13}$$

The *parabolic* scaling of space $x \in \mathbb{R}$ and time $t \geq 0$ with the *scale factor* $\lambda > 0$, namely the spatio-temporal transformation $\mathbb{P}_\lambda : x \mapsto \lambda x$ and $t \mapsto \lambda^2 t$, acts on a kink $k = q\delta_{x(t)}$, which occupies the location $x(t)$ at time t, by

$$(\mathbb{P}_\lambda \cdot k)(t) = q\delta_{\lambda x(\frac{t}{\lambda^2})}, \tag{14}$$

or equivalently, $q\delta_{x(t)} \overset{\mathbb{P}_\lambda}{\longrightarrow} q\delta_{\lambda x(\frac{t}{\lambda^2})}$. Given that the velocity $\mathcal{V}$, and the left- and right neighbour distances L_l and L_r, of a kink then transform respectively according to

$$\mathcal{V} \overset{\mathbb{P}_\lambda}{\longrightarrow} \frac{1}{\lambda}\mathcal{V}, \quad L_l \overset{\mathbb{P}_\lambda}{\longrightarrow} \lambda L_l\,, \quad L_r \overset{\mathbb{P}_\lambda}{\longrightarrow} \lambda L_r\,, \tag{15}$$

it immediately follows that $(\mathbb{P}_\lambda)_{\lambda \in (0,\infty)}$ furnishes a one parameter symmetry group of the kink dynamics (4): specifically, the *multiplicative group of positive reals* $\mathbb{R}^+ := \big((0,\infty), \cdot\big)$. Since the spin fractions are unaltered by $\mathbb{P}_\lambda$, the spin-excess σ is therefore conserved by it:

$$\sigma \overset{\mathbb{P}_\lambda}{\longrightarrow} \sigma. \tag{16}$$

There is yet another 1-parameter family of dynamical symmetries that covariantly acts on the distribution of distances between neighbouring kinks. But to discover it, we need to look outwith the original kink dynamics (4), since there it is *hidden* from view.

The Skew Neighbour Process ($\mathcal{SNP}$) . – The evolution of the distances between alternating kinks can be recast as a coarsening dynamical system of lengths. First, choosing to successively enumerate the kinks with integers $i \in \mathbb{Z}$, we denote the i^{th} kink's location by $x_i \in \mathbb{R}$, and its charge by $q_i \in \{\pm 1\}$. We adopt the convention of ordering the locations such that $x_i < x_{i+1}$, and also letting p-kinks (n-kinks) accrue an even (odd) index i, so that $q_i = (-1)^i$. The distances between successive kinks is then naturally encoded via the $\mathbb{Z}$-tuple of lengths $\mathfrak{l} := (\mathfrak{l}_i)_{i\in\mathbb{Z}}$, where $\mathfrak{l}_i := x_{i+1} - x_i$, with the corresponding $\mathbb{Z}$-tuple of domain-lengths at time t being denoted by $\mathfrak{l}[t]$, that is

$$\mathfrak{l}[t] := \big(\mathfrak{l}_i(t)\big)_{i\in\mathbb{Z}}. \tag{17}$$

The kink dynamics (4) may now be re-expressed purely in terms of the $\mathbb{Z}$-tuple of kink-locations $(x_i)_{i\in\mathbb{Z}}$,

$$\frac{\mathrm{d}x_i}{\mathrm{d}t} = (-1)^i \left(\frac{1}{x_i - x_{i-1}} - \frac{1}{x_{i+1} - x_i}\right). \tag{18}$$

Consequently, the temporal evolution of $\mathfrak{l}[t]$ is intrinsically governed, in the times between kink collisions, by the *skew nearest-neighbour* dynamical system

$$\frac{\mathrm{d}\mathfrak{l}_i}{\mathrm{d}t} = (-1)^i \left(\frac{1}{\mathfrak{l}_{i+1}} - \frac{1}{\mathfrak{l}_{i-1}}\right). \tag{19}$$

Furthermore, the ternionic coarsening motif exhibited in Fig. 3, which involves a pair of consecutive domain (facet) lengths shrinking to zero at some critical time t^*, naturally yields an associated coarsening update rule for $\mathfrak{l}[t^*]$, which, in fact, is expressible purely in terms of $\mathfrak{l}[t]$. Taking this intrinsic coarsening rule for $\mathfrak{l}[t]$, together with the length dynamics (19), one obtains a coarsening dynamical system for $\mathfrak{l}[t]$, which is henceforth referred to as the *Skew Neighbour Process* ($\mathcal{SNP}$).

The Hidden Dynamical Symmetry. The Skew Neighbour Process ($\mathcal{SNP}$) naturally inherits the symmetry group of the kink dynamics (4). In detail, $\mathbb{J}$ and $\mathbb{P}_\lambda$, which act on a $\mathbb{Z}$-tuple $\mathfrak{l} = (\mathfrak{l}_i)_{i\in\mathbb{Z}}$ by

$$(\mathbb{J}\cdot\mathfrak{l})_i := \mathfrak{l}_{1-i} \quad \text{and} \quad (\mathbb{P}_\lambda\cdot\mathfrak{l})_i(t) := \lambda\,\mathfrak{l}_i\left(\frac{t}{\lambda^2}\right), \tag{20}$$

each yield dynamical symmetries of (19). However, the $\mathcal{SNP}$ possesses an additional symmetry, which is not present in the original kink dynamics. Namely, the asymmetric scalings of lengths given by

$$\mathfrak{l}_{2i} \to a\mathfrak{l}_{2i} \quad \text{and} \quad \mathfrak{l}_{2i+1} \to \frac{1}{a}\mathfrak{l}_{2i+1}, \tag{21}$$

where $a > 0$. For future convenience, we reparametrise this one-parameter dynamical symmetry group of the $\mathcal{SNP}$ via the group action $\mathbb{T}_\varsigma$ on a $\mathbb{Z}$-tuple $\mathfrak{l} = (\mathfrak{l}_i)_{i\in\mathbb{Z}}$ defined by

$$(\mathbb{T}_\varsigma\cdot\mathfrak{l})_i := \begin{cases} a_\varsigma\mathfrak{l}_i & \text{if } i \text{ is even} \\ a_\varsigma^{-1}\mathfrak{l}_i & \text{if } i \text{ is odd}\end{cases}, \tag{22}$$

where $a_\varsigma := \sqrt{\frac{1+\varsigma}{1-\varsigma}}$, for each $\varsigma \in (-1, 1)$.

Statistical Mechanics of Kinks. – In what follows, let $\mathfrak{l} = (\mathfrak{l}_i)_{i\in\mathbb{Z}}$ be a non-periodic solution of the skew neighbour process ($\mathcal{SNP}$), whose lengths at the initial time $t = 0$ are uniformly small, $\mathfrak{l}_i[0] \ll 1$. By focusing attention on solutions with such a smallness condition at $t = 0$, we are thereby adopting a distinguished, albeit arbitrary, choice of *starting time*. We consider the *expectation* $\langle\ \rangle$ of the $\mathbb{Z}$-tuple $\mathfrak{l} = (\mathfrak{l}_i)_{i\in\mathbb{Z}}$, namely

$$L(t) := \langle\mathfrak{l}[t]\rangle, \tag{23}$$

which we henceforth refer to as the *characteristic length of the spin domains* L. In a similar fashion, the characteristic length of the spin-up domains L^+, and of the spin-down ones, L^-, are defined by

$$L^+(t) := \langle\mathfrak{l}^+[t]\rangle \quad \text{and} \quad L^-(t) := \langle\mathfrak{l}^-[t]\rangle, \tag{24}$$

where the $\mathbb{Z}$-tuples $\mathfrak{l}^+ := (\mathfrak{l}_{2i})_{i\in\mathbb{Z}}$ and $\mathfrak{l}^- := (\mathfrak{l}_{2i+1})_{i\in\mathbb{Z}}$ encode the lengths of the spin-up domains, and of the spin-down ones, respectively. The invariant spin-up and spin-down fractions, μ_+ and μ_-, now find expression through

$$\mu_+ = \frac{L^+}{L^+ + L^-} \quad \text{and} \quad \mu_- = \frac{L^-}{L^+ + L^-}. \tag{25}$$

Probing beyond the characteristic length L, we will also study the time-dependent probability density function (pdf) $P := \rho_\mathfrak{l}$, which encodes the distribution of the $\mathbb{Z}$-tuple of lengths $\mathfrak{l}[t] := (l_i(t))_{i\in\mathbb{Z}}$, being defined by

$$\int_\alpha^\beta \rho_\mathfrak{l}(l,t)\,\mathrm{d}l := \text{Prob}\left\{0 \le \alpha \le \mathfrak{l}[t] \le \beta\right\}, \tag{26}$$

where $\text{Prob}\{\alpha \le \mathfrak{l}[t] \le \beta\}$ denotes the probability that a randomly chosen length $l_i(t)$ from the $\mathbb{Z}$-tuple $\mathfrak{l}[t]$ lies between α and β. To characterise P, we will also need to study the spin-up and spin-down counterparts P^+ and P^-, which are associated with the $\mathbb{Z}$-tuples of spin-up (even) lengths, $\mathfrak{l}^+$, and spin-down (odd) lengths, $\mathfrak{l}^-$: i.e.,

$$P^+ := \rho_{\mathfrak{l}^+} \quad \text{and} \quad P^- := \rho_{\mathfrak{l}^-}. \tag{27}$$

Data obtained from the direct simulation of million-kink arrays (*kink ensembles*) strongly supports the premise that a *universal emergent statistical state* governs those ensembles with coincident spin-excess σ: see Figs. 5 and 6. We therefore hypothesise that any probability distribution of the domain lengths $\mathfrak{l}$ will universally adopt, after a temporal transient, a form depending solely on the spin-excess σ. This *Universality Hypothesis* ($\mathcal{UH}$) implies, in particular, the existence of the *spin-up (spin-down) σ-length* $\mathcal{L}_\sigma^+$ ($\mathcal{L}_\sigma^-$) and the *spin-up (spin-down) σ-distribution* ϱ_σ^+ (ϱ_σ^-) that capture, after a temporal transient, the behaviour of $L^\pm$ (24) and $P^\pm$ (27) respectively:

$$L^\pm \xrightarrow[\text{hypothesis}]{\text{universality}} \mathcal{L}_\sigma^\pm \quad \text{and} \quad P^\pm \xrightarrow[\text{hypothesis}]{\text{universality}} \varrho_\sigma^\pm. \tag{28}$$

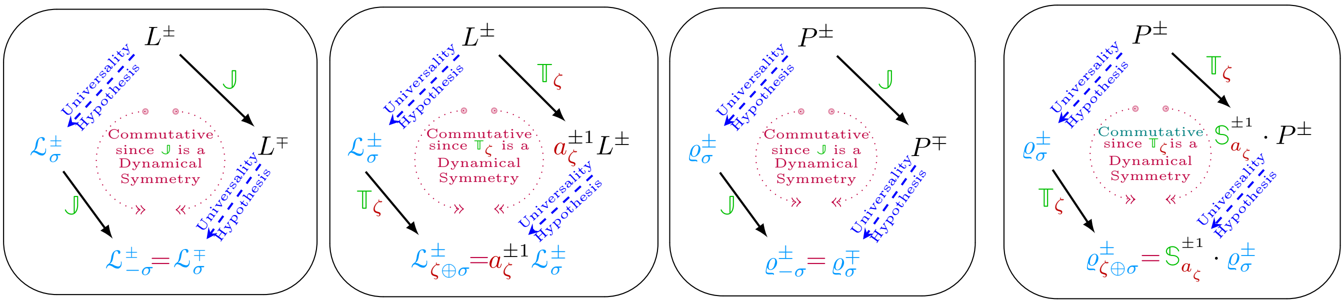

Fig. 4: Principle of G-Equivariant Universality: The symmetry-induced equivariance of the universal distributions $\mathcal{L}^{\pm}_{\sigma}$ and $\varrho^{\pm}_{\sigma}$ governing the skew neighbour process ($\mathcal{SNP}$), which follow from the particular dynamical symmetries $\mathbb{J}$ and $\mathbb{T}_\zeta$.

G-Equivariant Universality. – The group actions of inversion $\mathbb{J}$ (20), of parabolic scalings $\mathbb{P}_\lambda$ (20), and of *Lorentzian-boosts* $\mathbb{T}_\zeta$ (22), each commute with one another. Thus, the dynamical symmetry group of the Skew Neighbour Process ($\mathcal{SNP}$) includes the associated Cartesian-product group G: i.e.,

$$G = \mathbb{Z}_2 \times \mathbb{R}^+ \times ((-1,1), \oplus)\,. \tag{29}$$

We now verify that the spin-excess σ is *G-equivariant*. Given the $\mathbb{J}$- and $\mathbb{P}_\lambda$- equivariance of (13) and (16), it only remains to show that Lorentzian-boosts $\mathbb{T}_\zeta$ equivariantly transform the spin-excess σ. First, note that

$$L^{\pm} \xrightarrow{\mathbb{T}_\zeta} a_\zeta^{\pm 1} L^{\pm}, \tag{30}$$

and therefore

$$\frac{L^+}{L^-} \xrightarrow{\mathbb{T}_\zeta} a_\zeta^2 \frac{L^+}{L^-}. \tag{31}$$

But one also has

$$\frac{L^+}{L^-} = \frac{\mu_+}{\mu_-} = \frac{1+\sigma}{1-\sigma}, \tag{32}$$

which taken together with (31) yields

$$\frac{1+\sigma}{1-\sigma} \xrightarrow{\mathbb{T}_\zeta} a_\zeta^2 \frac{1+\sigma}{1-\sigma} = \left(\frac{1+\zeta}{1-\zeta}\right)\left(\frac{1+\sigma}{1-\sigma}\right) = \frac{1+(\zeta\oplus\sigma)}{1-(\zeta\oplus\sigma)}, \tag{33}$$

where $\oplus$ denotes the *Lorentzian addition* defined by

$$\zeta \oplus \sigma := \frac{\zeta+\sigma}{1+\zeta\sigma}. \tag{34}$$

The *Lorentz equivariance* of the spin-excess σ now follows directly from (33), namely, $\mathbb{T}_\zeta$ *boosts* σ by ζ:

$$\sigma \xrightarrow{\mathbb{T}_\zeta} \zeta \oplus \sigma. \tag{35}$$

By combining the universality hypothesis (28) with the *G-equivariance* of the spin-excess σ, we will now prove that $\mathcal{L}^{\pm}_{\sigma}$ and $\varrho^{\pm}_{\sigma}$ must, of necessity, also be G-equivariant. First, the inversion $\mathbb{J}$ exchanges spin-up and spin-down distributions, and so

$$L^{\pm} \xrightarrow{\mathbb{J}} L^{\mp} \quad \text{and} \quad P^{\pm} \xrightarrow{\mathbb{J}} P^{\mp}. \tag{36}$$

Furthermore, $\mathbb{J}$ also inverts the spin-excess σ (13), thus

$$\mathcal{L}^{\pm}_{\sigma} \xrightarrow{\mathbb{J}} \mathcal{L}^{\pm}_{-\sigma} \quad \text{and} \quad \varrho^{\pm}_{\sigma} \xrightarrow{\mathbb{J}} \varrho^{\pm}_{-\sigma}. \tag{37}$$

But $\mathbb{J}$ is also a dynamical symmetry of $\mathcal{SNP}$, and therefore the first and third diagrams in Fig. 4 commute, which in turn implies the inversion symmetries ($\mathbb{J}$-*equivariance*)

$$\mathcal{L}^{\pm}_{-\sigma} = \mathcal{L}^{\mp}_{\sigma} \quad \text{and} \quad \varrho^{\pm}_{-\sigma} = \varrho^{\mp}_{\sigma}. \tag{38}$$

Next, for the Lorentzian boost $\mathbb{T}_\zeta$, observe that

$$L^{\pm} \xrightarrow{\mathbb{T}_\zeta} a_\zeta^{\pm 1} L^{\pm} \quad \text{and} \quad P^{\pm} \xrightarrow{\mathbb{T}_\zeta} \mathbb{S}_{a_\zeta^{\pm 1}} \cdot P^{\pm}, \tag{39}$$

where the dilation operator $\mathbb{S}_a$ re-scales any given probability density P by $a > 0$, namely

$$(\mathbb{S}_a \cdot P)\,(l,t) := \frac{1}{a} P\left(\frac{l}{a}, t\right). \tag{40}$$

Note that $\mathbb{S}_{a^{-1}} = \mathbb{S}_a{}^{-1}$ (the inverse operator), and so $\mathbb{S}_{a_\zeta^{\pm 1}} = \mathbb{S}^{\pm 1}_{a_\zeta}$. Furthermore, since $\mathbb{T}_\zeta$ also *boosts* the spin-excess σ by ζ (35), one also finds that

$$\mathcal{L}^{\pm}_{\sigma} \xrightarrow{\mathbb{T}_\zeta} \mathcal{L}^{\pm}_{\zeta\oplus\sigma} \quad \text{and} \quad \varrho^{\pm}_{\sigma} \xrightarrow{\mathbb{T}_\zeta} \varrho^{\pm}_{\zeta\oplus\sigma}. \tag{41}$$

But again, $\mathbb{T}_\zeta$ is a dynamical symmetry of the $\mathcal{SNP}$, and so the second and fourth diagrams in Fig. 4 commute, which implies the Lorentzian equivariance ($\mathbb{T}_\zeta$-*equivariance*)

$$\mathcal{L}^{\pm}_{\zeta\oplus\sigma} = a_\zeta^{\pm 1}\mathcal{L}^{\pm}_{\sigma} \quad \text{and} \quad \varrho^{\pm}_{\zeta\oplus\sigma} = \mathbb{S}^{\pm 1}_{a_\zeta} \cdot \varrho^{\pm}_{\sigma}. \tag{42}$$

Last, for the parabolic scaling symmetry $\mathbb{P}_\lambda$, one finds

$$L^{\pm} \xrightarrow{\mathbb{P}_\lambda} \mathbb{P}_\lambda \cdot L^{\pm} \quad \text{and} \quad L^{\pm} \xrightarrow{\mathbb{P}_\lambda} \mathbb{P}_\lambda \cdot P^{\pm}, \tag{43}$$

where $(\mathbb{P}_\lambda \cdot L^{\pm})\,(t) := \lambda L^{\pm}\left(\frac{t}{\lambda^2}\right)$ and

$$\left(\mathbb{P}_\lambda \cdot P^{\pm}\right)(l,t) := \frac{1}{\lambda} P^{\pm}\left(\frac{l}{\lambda}, \frac{t}{\lambda^2}\right). \tag{44}$$

Also, σ is invariant under $\mathbb{P}_\lambda$ (16), and so

$$\mathcal{L}^{\pm}_{\sigma} \xrightarrow{\mathbb{P}_\lambda} \mathcal{L}^{\pm}_{\sigma} \quad \text{and} \quad \varrho^{\pm}_{\sigma} \xrightarrow{\mathbb{P}_\lambda} \varrho^{\pm}_{\sigma}. \tag{45}$$

Yet again, $\mathbb{P}_\lambda$ is a dynamical symmetry of the $\mathcal{SNP}$, and so by applying the rubrik of Fig. 4 with $\mathbb{P}_\lambda$, one obtains the parabolic invariance ($\mathbb{P}_\lambda$-*equivariance*)

$$\mathbb{P}_\lambda \cdot \mathcal{L}^{\pm}_{\sigma} = \mathcal{L}^{\pm}_{\sigma} \quad \text{and} \quad \mathbb{P}_\lambda \cdot \varrho^{\pm}_{\sigma} = \varrho^{\pm}_{\sigma}. \tag{46}$$

Beyond Scaling Laws. The G-equivariance exhibited in (38), (42) and (46) holds structural information on $\mathcal{L}_\sigma^\pm$ and $\varrho_\sigma^\pm$, which we now elucidate through a *group orbit calculation.* First, by considering the $\mathbb{J}$-equivariance (38) with $\sigma = 0$, one uncovers the natural symmetry

$$\mathcal{L}_0^+ = \mathcal{L}_0^-. \tag{47}$$

Combining this with the $\mathbb{P}_\lambda$-equivariance (46), one finds

$$\mathcal{L}_0^+(t) = \beta t^{\frac{1}{2}} = \mathcal{L}_0^-(t), \tag{48}$$

for some universal constant $\beta > 0$. Upon recalling the $\mathbb{T}_\zeta$-*equivariance* (42), one then discovers

$$\mathcal{L}_\sigma^\pm = a_\sigma^{\pm 1}\mathcal{L}_0^\pm = a_\sigma^{\pm 1}\beta t^{\frac{1}{2}}. \tag{49}$$

Given that the universality hypothesis ($\mathcal{UH}$) also implies

$$L \xrightarrow[\text{hypothesis}]{\text{universality}} \mathcal{L}_\sigma \quad \text{and} \quad P \xrightarrow[\text{hypothesis}]{\text{universality}} \varrho_\sigma, \tag{50}$$

it then follows, upon noting $L = \frac{1}{2}L^+ + \frac{1}{2}L^-$, that

$$\mathcal{L}_\sigma(t) = \frac{1}{2}\mathcal{L}_\sigma^+(t) + \frac{1}{2}\mathcal{L}_\sigma^-(t) = \frac{\beta}{\sqrt{1-\sigma^2}}\, t^{\frac{1}{2}}. \tag{51}$$

One may similarly prove that the spin-up and spin-down σ-distributions, namely ϱ_σ^+ and ϱ_σ^-, are not only *scale-invariant*, but remarkably assume a coincident σ-independent scaling form: i.e., there exists a universal normalised 1-point probability density function, here denoted by $\mathcal{W}(l)$, such that

$$\varrho_\sigma^\pm(l, \mathrm{t}) = \frac{1}{\mathcal{L}_\sigma^\pm(t)}\mathcal{W}\left(\frac{l}{\mathcal{L}_\sigma^\pm(t)}\right). \tag{52}$$

Furthermore, upon observing that $P = \frac{1}{2}P^+ + \frac{1}{2}P^-$ and $\frac{L^\pm}{L} = 1 \pm \sigma$, it readily follows from (28), (50) and (52) that the normalised domain-length distribution $\widehat{\varrho}_\sigma$ is time-independent, being given by a σ-weighted interpolation of $\mathcal{W}(l)$, namely

$$\widehat{\varrho}_\sigma(l,t) = \frac{1}{2}\frac{1}{1+\sigma}\mathcal{W}\left(\frac{l}{1+\sigma}\right) + \frac{1}{2}\frac{1}{1-\sigma}\mathcal{W}\left(\frac{l}{1-\sigma}\right). \tag{53}$$

Empirical Distributions. – The data taken from direct numerical simulation of the Skew Neighbour Process ($\mathcal{SNP}$), which is presented in Figs. 5 and 6, provides a robust validation of each of our theoretical predictions: namely, the coarsening law (51), the remarkable spin-excess independence and identity of the normalised spin-up and spin-down distributions (52), and the consequent interpolation prediction (53). When comparing the numerically computed pre-factor k in the parabolic scaling regime, $\langle \mathfrak{l}\rangle(t) = kt^{1/2}$, with the theoretical prediction of Eqn. (51), one notes a slight discrepancy as $\sigma \to 1^-$. But this is solely due to a numerical artefact, namely, the

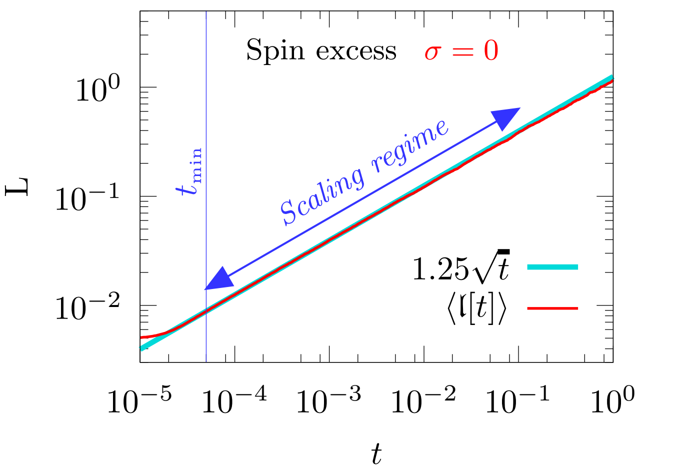

Fig. 5: Log-Log plot of the expected length $\langle \mathfrak{l}\rangle$ versus time t for a solution of the coarsening kink dynamics (4) starting from a slightly perturbed periodic alternating kink array with spin-excess $\sigma = 0$. After an initial temporal transient ($t > t_{\min}$) associated with the initial condition, the plot reveals the emergence of the parabolic scaling $\langle \mathfrak{l}\rangle = \beta t^{1/2}$ with $\beta \approx 1.25$.

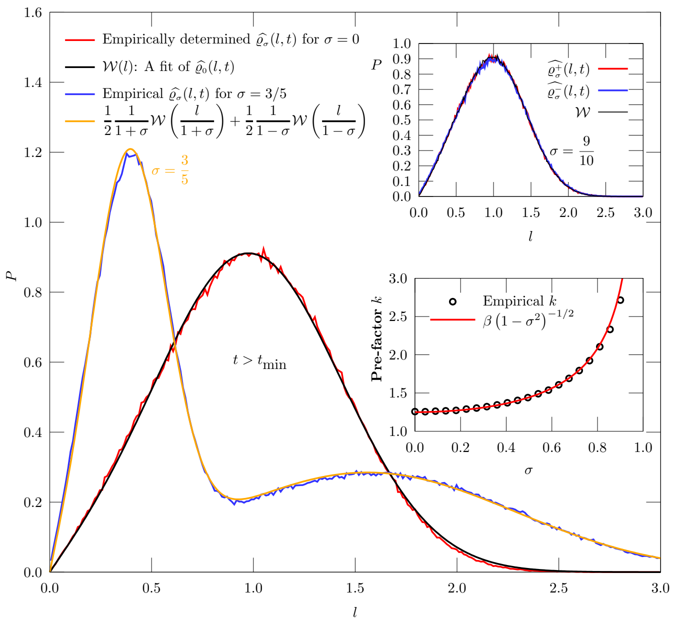

Fig. 6: The main figure presents the empirical probability distribution of normalised lengths, $\widehat{\varrho}_\sigma(l,t)$, obtained from ensembles of coarsening kinks with spin-excess $\sigma = 0$ and $\sigma = 0.6$, respectively. The probability density $\mathcal{W}(l)$ that is obtained from a least-squares fit of $\widehat{\varrho}_0(l,t)$ is also displayed, alongside a validation of the interpolation prediction (53) using it. The first insert demonstrates the coincidence of the numerically computed normalised spin-up and spin-down σ-distributions for $\sigma = 0.9$, namely $\widehat{\varrho_\sigma^+}(l,t) = \widehat{\varrho_\sigma^-}(l,t)$, while the second insert presents the variation with respect to σ of the numerically computed pre-factor k within the scaling regime $\langle \mathfrak{l}\rangle(\mathrm{t}) = kt^{1/2}$, and compares it to the predicted relativistic scaling appearing in Eqn. (51) with $\beta \approx 1.25$.

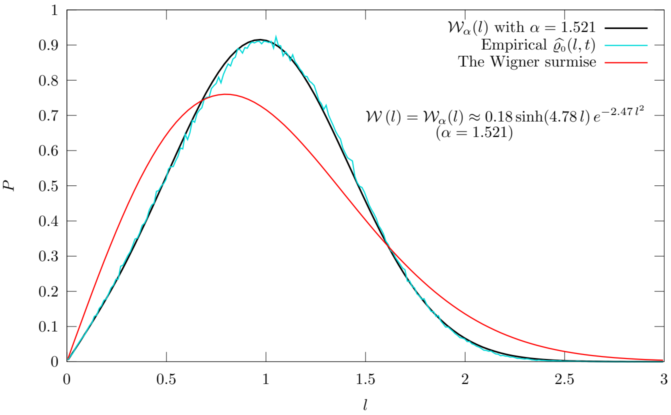

Fig. 7: Plot of $\mathcal{W}_\alpha(l)$ (54) with $\alpha \approx 1.521$ alongside the empirical probability distribution of normalised lengths $\widehat{\varrho}_0(l,t)$ obtained from direct simulation of million-kink ensembles.

stiffness of the dynamical system associated with the divergence of $\frac{1}{l}$ as $l \to 0^+$, which is accentuated when acquiring numerical data in the regime $\sigma \to 1^-$.

The probability distribution $\mathcal{W}(l)$ (52) is empirically determined from data derived from the numerical simulation of million-kink ensembles. We take $\mathcal{W}(l)$ to be the least-squares fit of our data (see Fig. 7) among the one-parameter family $\mathcal{W}_\alpha(l)$ of normalised probability functions

$$\mathcal{W}_\alpha(l) := \frac{2\alpha e^{-\alpha^2}}{\sqrt{\pi}\,[\operatorname{erf}\alpha]^2}\sinh\left(\frac{2\alpha^2 l}{\operatorname{erf}\alpha}\right)\exp\left(-\frac{\alpha^2 l^2}{[\operatorname{erf}\alpha]^2}\right), \tag{54}$$

where $\alpha \in (0,\infty)$, $\operatorname{erf}\alpha := \frac{2}{\sqrt{\pi}}\int_0^\alpha e^{-s^2}\mathrm{d}s$ (the *error function*), while $\int_0^\infty \mathcal{W}_\alpha(l)\mathrm{d}l = 1 = \int_0^\infty l\mathcal{W}_\alpha(l)\mathrm{d}l$, by design. Given that the asymptotic structure of $\mathcal{W}_\alpha(l)$ as $\alpha \to 0^+$ yields precisely the *Wigner surmise*, namely

$$\lim_{\alpha\to 0^+}\mathcal{W}_\alpha(l) = \frac{\pi}{2}l\,e^{-\frac{\pi}{4}l^2}, \tag{55}$$

this α-family $\mathcal{W}_\alpha(l)$ may be naturally viewed as a hyperbolic deformation of the Wigner surmise.

The remarkable supra-universal theoretical prediction (52) for the $\mathcal{SNP}$ has also previously been empirically observed by Cornell & Bray [18] for the conservative (Kawasaki) dynamics of Ising-spin chains subject to a weak (*symmetry-breaking*) field: namely, the scaling form of the spin-up and the spin-down domain-length distributions were found, by direct numerical simulation, to be identical and independent of the invariant spin fractions $\mu_\pm$. Furthermore, by assuming this supra-universality, while also relying on further *closure hypotheses*, Cornell & Bray also attempted to theoretically predict the dependence of the characteristic domain length on the spin (*phase*) fractions $\mu_\pm$, as well as the *scaling function* for the domain sizes in the *"off-critical"* limit $\mu_+ \to 0^+$. However, in each case, their closure hypotheses are inconsistent with the conservation of spin fractions. This point is, in fact, explicitly conceded within said paper (page 1157 of [18]), where the authors place the disclaimer that their "calculation is only valid to lowest order in" μ_+. Be that as it may, the coincident supra-universal behaviour (52) of both models is an astonishing fact, beyond reproach. We therefore conjecture that the *emergent hydrodynamic* (continuum) limit of the weakly driven kinetic Ising model treated in [18] is necessarily the conservative spin model given by Eqns. 5 and 6, wherein the requisite explanatory hidden Lorentzian boost sits.

Conclusion. – We have discovered how the dynamical symmetry group G of a Coarsening Dynamical System ($\mathfrak{CDS}$) covariantly (equivariantly) acts on that $\mathfrak{CDS}$'s universal emergent parameters and probability distributions. We exhibit this *G-Equivariant Universality* for a model chiral $\mathfrak{CDS}$, whose Lorentzian-parabolic dynamical symmetries permit us to theoretically predict a universal coarsening law that goes beyond mere scaling. It has not escaped our attention that the G-equivariant theory of coarsening (ageing) developed herein parallels Wilson's renormalisation-group theory for scale-invariance (conformal invariance) of *critical phenomena* [19]. In this vein, we propose the *Principle of G-Equivariant Universality*, concisely illustrated in Fig. 4, to be the natural generalisation of the *dynamic scaling hypothesis*, anticipating that it will find resonance and application well beyond the confines of the particular coarsening (ageing) system considered here.

REFERENCES

[1] BRAY A. J., *Adv. Phys.* **43** (3) (1994) 357.
[2] SCHITTMANN B. & ZIA R. K. P., Statistical Mechanics of Driven Diffusive Systems (Academic Press)1995.
[3] ALLEN S. M. & CAHN J. W., *Acta Metal.* **27** (1979) 1085.
[4] MULLINS W. W., *J. Appl. Phys.* **59** (1986) 1341
[5] ROSS F. M. *et al*, *Phys. Rev. Lett.* **80** (1998) 984.
[6] SADLER L. E. *et al*, *Nature* **443** (2006) 312.
[7] WATSON S. J. & NORRIS S. A., *Phys. Rev. Lett.* **96** (2006) 176103.
[8] MacPHERSON R. D. & SROLOVITZ D. J., *Nature* **446** (2007) 1053.
[9] De SILVA M. S. *et al*, *P. Natl. Acad. Sci. USA* **108** (2011) 9408.
[10] BARNAK K. *et al*, *Phys. Rev. B* **83** (2011) 134117.
[11] PARK H. & PLEIMLING M., *Eur. Phys. J. B* **85** (2012) 300.
[12] WITTKOWSKI R. *et al*, *Nature Communications* **5** (2014) 4351
[13] WATSON S. J., *Proc. R. Soc. A* **471** (2015) 20140560.
[14] GODRECHE C. & DROUFFE J.-M., *J. Phys. A: Math. Theor.* **50** (1) (2016) 015005
[15] HOHENBERG P. C. & HALPERIN B. I., *Rev. Mod. Phys.* **49** (1977) 435.
[16] PAPANIKOLAOU S. *et al.*, *Nature Physics* **7** (2011) 316.
[17] HENKEL M. & PLEIMLING M., Non-Equilibrium Phase Transitions, (Springer) 2010.
[18] CORNELL S. J. & BRAY A. J., *Phys. Rev. E* **54** (1996) 1153.
[19] WILSON K. G., *Rev Mod. Phys.* **55** (1983) 583.